Sociedade Brasileira de Automática (SBA)
XXIV Congresso Brasileiro de Automática - CBA 2022, 16 a 19 de outubro de 2022

Small-signal model for stability analysis of different microgrid configurations ⋆

Gustavo C. M. Oliveira * **Reginaldo V. Ferreira** * **Sidelmo M. Silva** ** **Leandro Freitas** *

* *Instituto Federal de Minas Gerais, IFMG, Betim, MG (e-mails: gustavocesar.mo@gmail.com, reginaldo.ferreira@ifmg.edu.br, leandro.freitas@ifmg.edu.br)*
** *Universidade Federal de Minas Gerais, UFMG, Belo Horizonte, MG (e-mail: sidelmo@ufmg.br)*

Abstract: The expansion of distributed generation in the context of microgrids has allowed the emergence of increasingly larger and more complex structures, with different amounts of converters and control techniques, different operating modes, presence of local loads, among others. In this context, the development of models to analyze the stability of microgrids provides an important tool for greater assurance of a safe and efficient operation. Thus, the objective of this paper is to propose a modular small-signal model, capable to represent different configurations of microgrids, for system stability analysis. As a case study is presented a microgrid with two converters, using two different control techniques: droop and synchronverter, with local loads and operating in connected mode. The paper validates the developed small-signal model, through the comparison with the behavior of a dynamic model simulated in MATLAB/Simulink, and presents stability analysis in relation to the controllers gains.

Keywords: Distributed generation, microgrids, small-signal model, droop control, synchronverter, stability analysis.

1. INTRODUCTION

In recent years, the demand for renewable energy generation has increased considerably, mainly for economic and environmental reasons, with a greater search for alternatives to replace fossil fuel resources (Borazjani et al., 2014) and to diversify energy generation. In this context, the idea of distributed generation (DG) has been widely discussed, in which electrical sources locally, such as photovoltaic power plants and wind turbines, provide electrical energy for local loads (Vechiu et al., 2011). The possibility of integrating distributed generation units became viable with the concept of microgrids, which allows the interconnection between sources, loads and storage elements (Saeed et al., 2021).

Microgrids can operate in two conditions: connected mode, when the generating units exchange energy with the main grid, and isolated mode, in which these units are responsible for maintaining the integrity of the grid without the assistance of a main grid (Zhou et al., 2020). Regardless of the operating mode, it is notable that there is a need for interfaces between DG units to form a microgrid and make possible the connection to a main grid (Vechiu et al., 2011), since most of the distributed/renewable-energy generators correspond to different forms of generation, such as: variable-frequency AC sources, high-frequency AC sources, or DC sources (Zhong and Weiss, 2011).

⋆ This work was financially supported by the Instituto Federal de Minas Gerais.

With the large number of converters present in a microgrid, the control method becomes essential to ensure stability and power quality. There are different converter control techniques, some of which allow converters to share loads or supply power together with the main grid without communication (Borazjani et al., 2014). In this sense, it is possible to highlight: the droop control, already consolidated in the literature, and the synchronverter, that has received attention among researchers. These two techniques have in common the idea of emulating a synchronous machine (Ferreira et al., 2016; Zhong and Weiss, 2011).

Considering the entire context of a microgrid, which ranges from the control used in a simple converter to the entire structure, stability analysis becomes very important to understand better the essential characteristics for safe and efficient operation. Most of the stability analysis have been focused on small-signal modelling in conjunction with linearization methods, which is valid around an equilibrium point (Konstantopoulos et al., 2014) and, in general, models found in the literature are developed for a specific microgrid configuration.

This paper proposes a modular small-signal model, which allows different microgrid configurations, in terms of operating mode (connected or isolated), number of converters, use of different control techniques and presence or absence of local loads, making it easier to carry out changes in the structure without the need to change the entire model. To validate the proposed model, a microgrid configuration is defined as a case study, with: two converters, controlled by two different control techniques (droop and synchron-

verter), operating in connected mode and with the presence of local loads. The model is analyzed numerically and the main characteristics are discussed.

2. A BRIEF REVIEW ON CONVERTERS EMULATING SYNCHRONOUS MACHINES

Figure 1 presents the converter with its power and control parts. In the power part, a primary source, such as photovoltaic or wind power, is shown, connected to the input of a DC-AC converter, which has an LC filter at its output, represented by L_f and C_f. This converter is connected to the grid, with a Z_g line impedance. The converter control is implemented with the calculation of the active and reactive powers, from the voltage and current measurements, and then these powers are controlled. The output of the PQ control loops provides the setpoints for the inner voltage and current control loops, which, finally, generate the references for the PWM (Pulse Width Modulation), responsible for driving the static power devices of the converter.

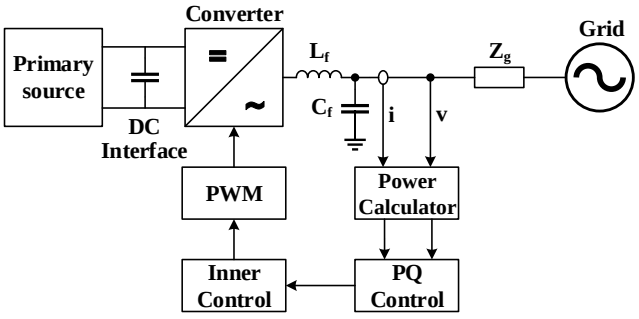

Figure 1. Power and control parts present in a converter, showing the voltage and current (inner) control, the external active (P) and reactive (Q) power control, and the interactions with a primary source and the grid.

Control techniques that emulate the behavior of synchronous machines represent a viable possibility of decentralized control for the parallel connection of converters. These techniques have some advantages, such as: possibility of independent control of reactive and active power injection, ability to operate converters in parallel with different nominal parameters, easy power sharing capability, among others (Ferreira, 2019).

Subsections 2.1 and 2.2 present a basic review of droop and synchronverter control methods, respectively.

2.1 Droop Control

Droop control is the most popular method for power sharing between sources in a microgrid (Wandhare et al., 2014). It is based on the idea that, even though the flow of active and reactive powers in a system are not decoupled, active power mainly depends on frequency and reactive power mainly depends on voltage amplitude, considering a predominantly inductive grid (Coelho, 2000). Thus, the frequency and voltage control is achieved through the active and reactive powers respectively, as shown in (1) and (2).

$$\omega = \Omega^* - k_p(P_f - P^*), \quad (1)$$
$$v = V^* - k_q(Q_f - Q^*), \quad (2)$$

where Ω^* and V^* are the angular frequency and magnitude voltage references, k_p and k_q are the droop coefficients, the P_f and Q_f terms are the measured average active and reactive powers, obtained through voltage and current measurements and calculated in the dq reference. P^* and Q^* represent the active and reactive power setpoints (Wang et al., 2020).

It is important to mention that different configurations are required depending on the operating conditions. Figure 2 illustrates the droop control with these configurations.

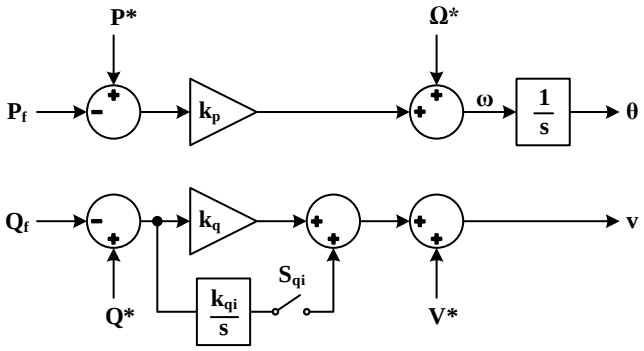

Figure 2. Block diagram with different settings of droop control, with or without integral action in reactive power loop, depending on S_{qi} switch.

When the microgrid operates in connected mode, the converter must supply the selected values of active and reactive powers, P^* and Q^*, without significant steady state errors. In the frequency control loop, shown in the top of Figure 2, the presence of the integrator ensures zero steady state error. However, in the voltage control loop, the integrator is not naturally used, allowing errors to occur in the supply of the desired reactive power, considering the connected operating mode. Therefore, in this case, it is necessary to add it to the loop, in parallel with gain K_q, and the integrator gain K_{qi} must be properly chosen, according to the power supply definitions. This insertion can be done by closing the S_{qi} switch, which adds this element to the voltage loop.

In isolated mode, the focus becomes on controlling voltage magnitude and frequency, not being necessary to correct steady state errors of active and reactive powers. In this case, the integrator in the voltage loop is no longer useful and needs to be removed, by opening the S_{qi} switch in Figure 2.

2.2 Synchronverter

The synchronverter algorithm originated from the idea of converters that mimic synchronous generators, introduced in Zhong and Weiss (2011). A synchronverter can be basically divided into a power part, composed of the converter itself and LC filters, and a control part, where there is the mathematical model of a three-phase round-rotor synchronous machine (Zhong et al., 2014). Figure 3 illustrates the control part.

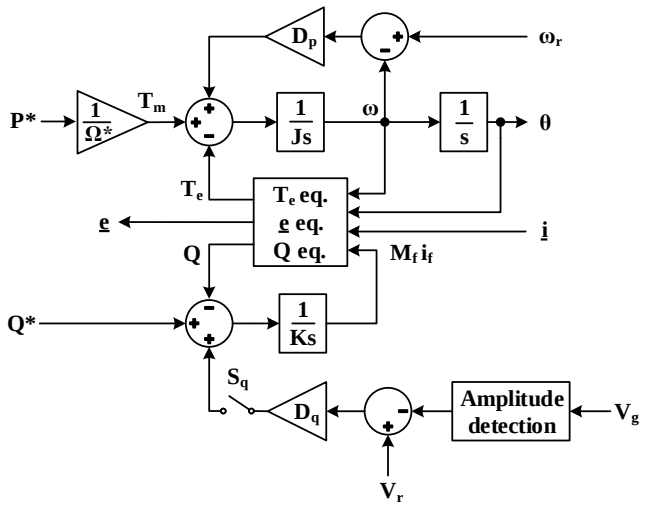

Figure 3. Block diagram with different settings of the synchronverter, with or without the effect of the difference between V_r and V_g, depending on S_q switch.

The three equations in the central block of Figure 3 represent the electromagnetic torque (T_e), the output voltage ($\underline{e}$) or, in other words, the induced voltage of the virtual machine, and the reactive power (Q).

$$T_e = M_f i_f \langle \underline{i}, \sin(\underline{\theta}) \rangle, \tag{3}$$
$$\underline{e} = \omega M_f i_f . \sin(\underline{\theta}), \tag{4}$$
$$Q = -\omega M_f i_f \langle \underline{i}, \cos(\underline{\theta}) \rangle. \tag{5}$$

M_f and i_f are the mutual inductance and the rotor excitation current, respectively; ω is the frequency; $\langle \cdot, \cdot \rangle$ represents the conventional inner product, in $\mathbb{R}^3$, and $\sin(\underline{\theta})$ and $\cos(\underline{\theta})$ are:

$$\sin(\underline{\theta}) = \begin{bmatrix} \sin(\theta) \\ \sin(\theta - 2\pi/3) \\ \sin(\theta + 2\pi/3) \end{bmatrix}, \cos(\underline{\theta}) = \begin{bmatrix} \cos(\theta) \\ \cos(\theta - 2\pi/3) \\ \cos(\theta + 2\pi/3) \end{bmatrix}.$$

In addition to these terms, inputs i and V_g receives the current and voltage, measured at the converter output, and ω_r and V_r are the angular frequency and magnitude voltage references. P^* and Q^* are the active and reactive power setpoints. The coefficients D_p and D_q represent the damping factor of a synchronous machine and the voltage-droop coefficient, respectively, and the term K defines the gain of the integrator in the voltage-droop control loop. All these mentioned terms are better described and explored in Zhong and Weiss (2011).

This control technique is very similar to the droop control, with the same strategy of controlling power through adjustment of frequency and voltage amplitude. The most relevant difference is that, in the synchronverter, there is a virtual inertia, represented by the term J in Figure 3 (Liu et al., 2015). One advantage is that when a synchronverter is connected to the grid, no significant difference is felt by the grid, compared to a synchronous generator. This allows the usage of the same control algorithms commonly used in power systems (Wei et al., 2015).

An important feature is that the reactive power delivered by the synchronverter, considering its original structure and operation in connected mode, presents a steady state error. In this sense, Zhong et al. (2014) proposes, among other adaptations, a solution to overcome this problem, which consists of adding the S_q switch, present in Figure 3. When the switch is opened, $M_f i_f$ is generated only by the difference between the power setpoint and the measured power, without the influence of the difference between V_r and V_g. This guarantees null error for the reactive power, with greater precision in the delivery of the requested power.

3. SMALL-SIGNAL MODELS APPLIED TO ISOLATED AND GRID-CONNECTED POWER SYSTEMS

There are several examples in the literature of small-signal models applied to distributed generation or microgrids. Considering an AC microgrid, the configurations vary, generally, in relation to the operating mode (connected or isolated), quantity of converters, converter control technique, the presence or absence of local loads, also with differences between the type of load. In this context, there are different model structures, which can be modular or fixed, in the sense of allowing or not changes in the structure.

Table 1 gathers the main characteristics of models developed in some references (Cao et al., 2014; Coelho et al., 2002; Ferreira et al., 2019; Liu et al., 2020; Rodríguez-Cabero et al., 2017; Vetoshkin and Müller, 2020; Wei et al., 2015; Yu et al., 2015), with different configurations and structures.

Table 1. Characteristics of small-signal model references.

Reference	Modular	Control	Mode
Cao et al.	No	Droop	Isolated
Coelho et al.	No	Droop	Isolated
Ferreira et al.	Yes	Droop/ Synchron.	Connected
Liu et al.	No	Droop	Isolated
Rodríguez-Cabero et al.	No	Synchron.	Isolated
Vetoshkin and Müller	No	Synchron.	Isolated
Wei et al.	No	Synchron.	Connected
Yu et al.	No	Droop	Connected

In almost all the cited examples, the models were developed through state-space representation, which despite having different configurations, do not present modularity, that is, do not easily allow modifications of the structure.

In this sense, the small-signal model shown in Ferreira et al. (2019) is represented in a different way, in the Laplace domain, in which each part of the system is presented in its own matrix, with a modular aspect. However, its modularity is explored only in the possibility of modifying the control technique through the exchange of a matrix.

The main idea of the present work is to further explore the model obtained by Ferreira et al. (2019), presenting a model structure where it is possible to modularly represent microgrids with different configurations, being able to operate in isolated or connected mode.

4. A MODIFIED MODULAR SMALL-SIGNAL MODEL FOR DIFFERENT MICROGRID CONFIGURATIONS

The modeling developed by Ferreira et al. (2019) presents the entire structure of a converter connected to a main grid

divided into blocks of transfer matrices, which linearize the non-linear behavior present in many parts of the structure. In that case, the main idea is to obtain a unified structure that allows modifying the control technique through the exchange of a single 2×2 matrix, in order to mainly compare the dynamic operation of the droop control and the synchronverter. This structure is shown in Figure 4, and can be basically divided into three parts: line impedance, present between the converter and the main grid; representation of frequency variations, which generate effects on line impedance, and the converter together with the control loops, which range from power measurement to the generation of the reference voltage.

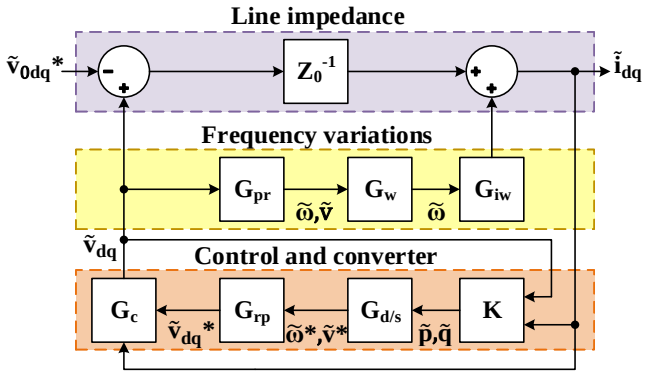

Figure 4. Block diagram of the small-signal model (Adapted from Ferreira et al., 2019).

Each block presented in Figure 4 represents a specific part of the model and is better described and shown in Table 2.

R and L are the line resistance and inductance, and are also important for calculating the impact of frequency variation. V_d, V_q, I_d and I_q represent the operating points of the converter output voltage and current, all in the dq reference frame. In the droop control matrix, the w_f term is present, representing the cut-off frequency of the power measurement low-pass filter. V and Ω are the operating points of converter output voltage magnitude and system frequency. All these terms shown in Table 2 can be better understood in Ferreira et al. (2019), which inserts and introduces them during modeling development.

The Gc block, shown in Figure 4, represents the ratio between the output voltage and the reference voltage of the converter, having in its structure the inner voltage and current control loops. Considering that these loops are faster when compared to external power control loops, and therefore practically do not influence the system dynamics, this Gc block was disregarded in this work, not being shown in Table 2, reducing the complexity of development and analysis.

The model obtained by Ferreira et al. (2019) was applied in two distinct microgrids, one using droop control technique and other using synchronverter. However, the model was not applied to a microgrid that involves, simultaneously, both control techniques. In the present work, the model proposed by Ferreira et al. (2019) was extended, highlighting the modularity and flexibility capabilities of the model to different microgrids configurations. The performance of the modeling is validated in a microgrid with two converters using two different control techniques, droop and synchronverter, operating in connected mode and with the presence of local loads.

Figure 5 illustrates the structure defined for this work, which brings the idea of having a flexible microgrid, regarding the operating mode, possibility of connecting local loads, number of converters and types of control techniques.

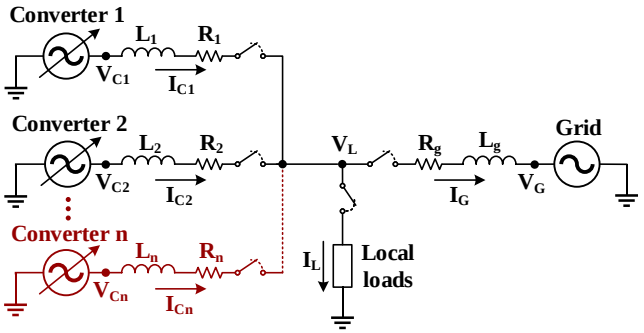

Figure 5. Flexible representation of a microgrid for different configurations: connected or isolated mode, with/without local loads and with a variable number of converters and control techniques.

To obtain the small-signal model of the microgrid in Figure 5, it is necessary to obtain the equations that basically involve the voltages and currents, which are the inputs/outputs of the model blocks, in addition to the impedance of each part. In Figure 5 the current load I_L is given by

$$I_L = I_{C1} + I_{C2} + ... + I_{Cn} - I_G, \tag{6}$$

where $I_{C1}, I_{C2}, \ldots, I_{Cn}$ are the converters currents and I_G the current supplied to the main grid. The load voltage V_L is given by the Ohm's law

$$V_L = Z_L I_L, \tag{7}$$

where Z_L is the load impedance. The current coming from any of the converters is given by

$$I_{Cx} = (V_{Cx} - V_L) {Z_{Cx}}^{-1}, \tag{8}$$

where the index x represents a specific converter, with V_{Cx} and Z_{Cx} being their respective output voltage and line impedance.

The reasoning for calculating the current from the microgrid to the main grid is exactly the same, being calculated through

$$I_G = (V_L - V_G) {Z_G}^{-1}, \tag{9}$$

where V_G and Z_G are the main grid voltage and line impedance.

When the main grid operates helping the converters to supply the loads, the only difference will be in the modification of the signs of the current I_G and the voltages V_L and V_G in (6) and in (9), respectively.

In the next section, the modeling procedure presented so far is validated through the case study of a specific microgrid configuration.

Table 2. Description and representation of the small-signal model blocks by Ferreira et al. (2019)

Block	Description	Matrix
Z_0	Line impedance	$\begin{bmatrix}(sL+R) & -\Omega L \\ \Omega L & (sL+R)\end{bmatrix}$
K	Power measurement	$\frac{3}{2}\begin{bmatrix}V_d & V_q \\ V_q & -V_d\end{bmatrix}\begin{bmatrix}\tilde{i}_d \\ \tilde{i}_q\end{bmatrix} + \frac{3}{2}\begin{bmatrix}I_d & I_q \\ -I_q & I_d\end{bmatrix}\begin{bmatrix}\tilde{v}_d \\ \tilde{v}_q\end{bmatrix}$
G_d	Droop gains and low-pass filter	$\begin{bmatrix}-K_p\frac{\omega_f}{s+\omega_f} & 0 \\ 0 & -K_q\frac{\omega_f}{s+\omega_f}\end{bmatrix}$
G_s	Synchronverter	$\begin{bmatrix}-\frac{1}{\Omega}\frac{1}{(sJ+D_p)} & 0 \\ \frac{\Lambda_f}{\Omega}\frac{1}{(sJ+D_p)} & -\frac{1}{(\frac{sK}{\Omega}+D_q)}\end{bmatrix}$
G_{rp}	Reference voltage	$\begin{bmatrix}-\frac{V_q}{s} & \frac{V_d}{V} \\ \frac{V_d}{s} & -\frac{V_q}{V}\end{bmatrix}$
G_{pr}	Converter output voltage and frequency	$\begin{bmatrix}V_q \cdot s & V_d \cdot s \\ V_d \cdot V & V_q \cdot V\end{bmatrix}$
G_w	Frequency variation	$\begin{bmatrix}1 & 0\end{bmatrix}$
G_{iw}	Impact of frequency variation	$\begin{bmatrix}\frac{-(s+\frac{R}{L})I_q - \Omega Id}{(s+\frac{R}{L})^2+\Omega^2} \\ \frac{(s+\frac{R}{L})I_d - \Omega Iq}{(s+\frac{R}{L})^2+\Omega^2}\end{bmatrix}$

5. PROPOSAL AND VALIDATION OF THE MODULAR SMALL-SIGNAL MODEL

To validate the proposed modular small-signal model, a microgrid structure was defined for a case study, with: two converters, local loads and operating in connected mode. A control technique was determined for each converter, with droop control for one and synchronverter for the other, which represents a characteristic not explored by any of the references mentioned in Table 1.

The block diagram of the proposed model is shown in Figure 6.

As mentioned before, the inner voltage and current control loops were not considered in the model, defining the G_c block, shown in Figure 4, as a unity gain for the voltage input and zero gain for the current input. This was done for both converters. In addition, the control matrices were modified in the model shown in Figure 6, in relation to those presented in Table 2, adding the integrator in parallel with the gain K_q, in the droop control of converter 1, as shown in subsection 2.1, and removing the effect of the difference between the voltages in the voltage loop, in the synchronverter of converter 2, as shown in subsection 2.2.

In order to validate the small-signal model of the proposed microgrid, a dynamic model was implemented in MATLAB/Simulink with the same structure, to compare the behavior of both models. Table 3 presents the parameters used for the simulations.

Table 3. Simulation parameters.

Parameters	Value	Unit
Grid		
Voltage magnitude (V_G)	$127\sqrt{2}$	V
Frequency (f_G)	60	Hz
Line resistance (R_G)	6	$m\Omega$
Line inductance (L_G)	5.34	μH
Local loads		
Active power (P_L)	5	kW
Reactive power (Q_L)	2.5	$kVAr$
Converter 1 (droop control)		
Line resistance (R_1)	0.33	Ω
Line inductance (L_1)	48	μH
Coupling inductance (L_{c1})	1.56	mH
Output active power (P_1)	6	kW
Output reactive power (Q_1)	3	$kVAr$
Frequency droop gain (K_p)	$5.24 \cdot 10^{-4}$	$(rad/s)/W$
Voltage droop gain (K_q)	$2.99 \cdot 10^{-3}$	V/VAr
Voltage loop integrator gain (K_{qi})	0.4	-
Low-pass filter frequency (ω_f)	6	Hz
Converter 2 (synchronverter)		
Line resistance (R_2)	0.37	Ω
Line inductance (L_2)	32.5	μH
Coupling inductance (L_{c2})	2.34	mH
Output active power (P_2)	4	kW
Output reactive power (Q_2)	2	$kVAr$
Damping factor (D_p)	3.38	$N \cdot m/(rad/s)$
Voltage-drooping coefficient (D_q)	222.71	VAr/V
Virtual moment of inertia (J)	$8.96 \cdot 10^{-3}$	$kg \cdot m^2$
Voltage loop integrator gain (K)	2227.11	VAr/V

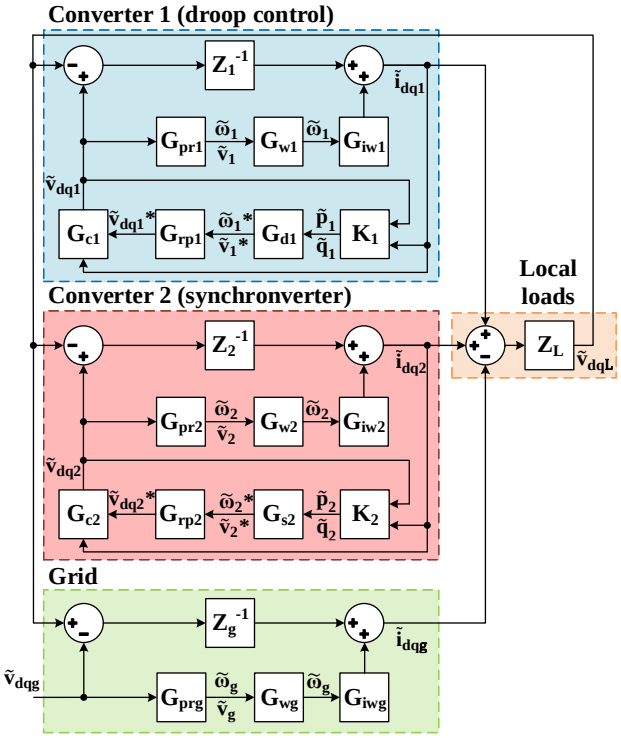

Figure 6. Block diagram of the microgrid proposed for a case study, with: two converters, each with a control technique (droop and synchronverter), local loads and operating in connected mode.

For validation, output frequency and current in the d-axis variations were evaluated for each converter, applying a 5% voltage sag disturbance in the d-axis voltage of the main grid, during 50 ms. Figures 7a and 7b show the results obtained for converter 1 and figures 8a and 8b for converter 2, both for the dynamic model and for the small-signal model.

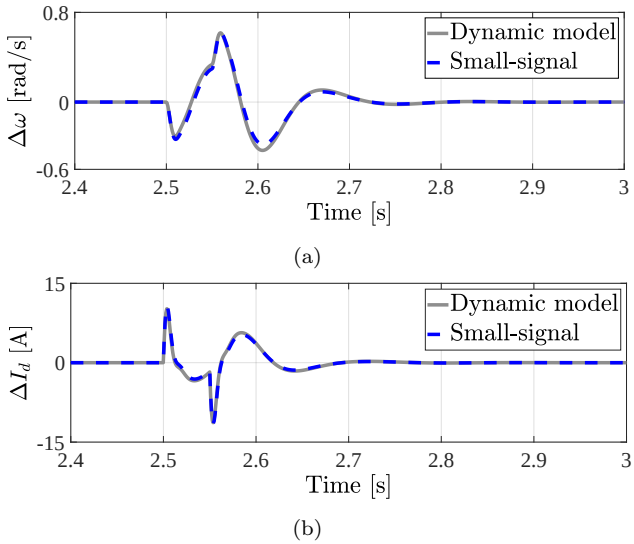

Figure 7. Dynamic behavior in converter 1 (droop control), under a 5% sag disturbance at the main grid d-axis voltage for 50 ms, of: (a) frequency variation and (b) d-axis current variation.

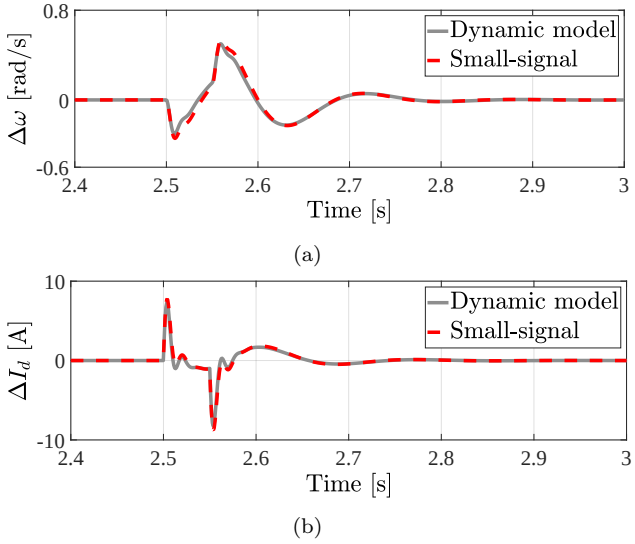

Figure 8. Dynamic behavior in converter 2 (synchronverter), under a 5% sag disturbance at the main grid d-axis voltage for 50 ms, of: (a) frequency variation and (b) d-axis current variation.

As it can be seen in Figures 7a, 7b, 8a and 8b, the dynamics in both models were close, with minimal differences between them. Although the results of the operation in isolated mode are not shown in this work, due to page limits, the small-signal model was also validated in this mode, presenting a similar performance with that observed in the connected mode.

The possibility of working with a linear model, as is the case here, presents the advantage of having several stability analysis tools available, and this approach is explored in the next topic. A relevant consequence of linearization is that the model performance depends on how close to the operating points it is being used. The further away from the operating points, lower the performance. In this sense, it is clear the importance of considering that the small-signal model will represent the real system in an approximate way. Thus, a model can have a more conservative representation, indicating smaller margins for parameter variation, or a less conservative representation, where the real system has smaller margins, compared to the small-signal model. In all cases, it is more interesting to obtain a more conservative model, which ensures stability for the indicated limits.

5.1 Stability Analysis

To analyze the stability of the established microgrid configuration, through the small-signal model, the position of the system poles in the complex plane was evaluated during the variation of the controllers gains, in order to obtain the stability limits of the microgrid for the adjusted parameters. Figure 9 shows the system poles with the parameters of Table 3, in which the system is stable.

Figures 10a, 10b, 11a and 11b show the small-signal model poles in the complex plane, in an enlarged form, during the variation of gains K_p and K_q, of the droop control, and D_p and D_q, of the synchronverter, respectively, showing the gain limit where the system ceases to be stable and

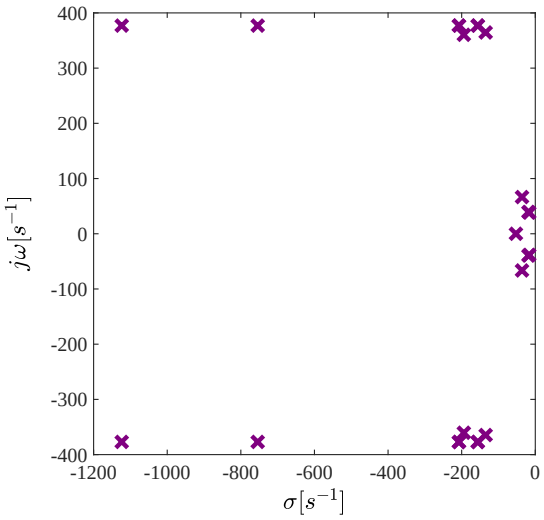

Figure 9. Poles of the small-signal model with the defined parameters.

becomes unstable. To verify the results, the frequency, obtained in the dynamic model, is presented for the converter where the gain has been changed, with a variation of 10% around the limit value obtained, that is, with a gain of 5% lower than the limit and with a 5% higher gain.

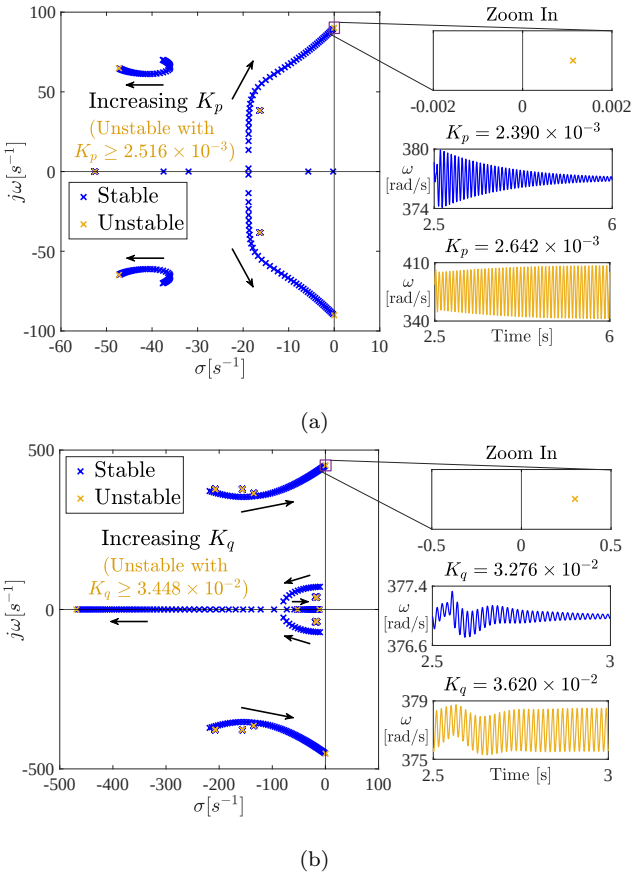

Figure 10. Small-signal model poles in the complex plane during (a) K_p gain variation and (b) K_q gain variation, and dynamic model frequency in converter 1 (droop control) with 10% variation around the (a) K_p limit for instability and (b) K_q limit for instability.

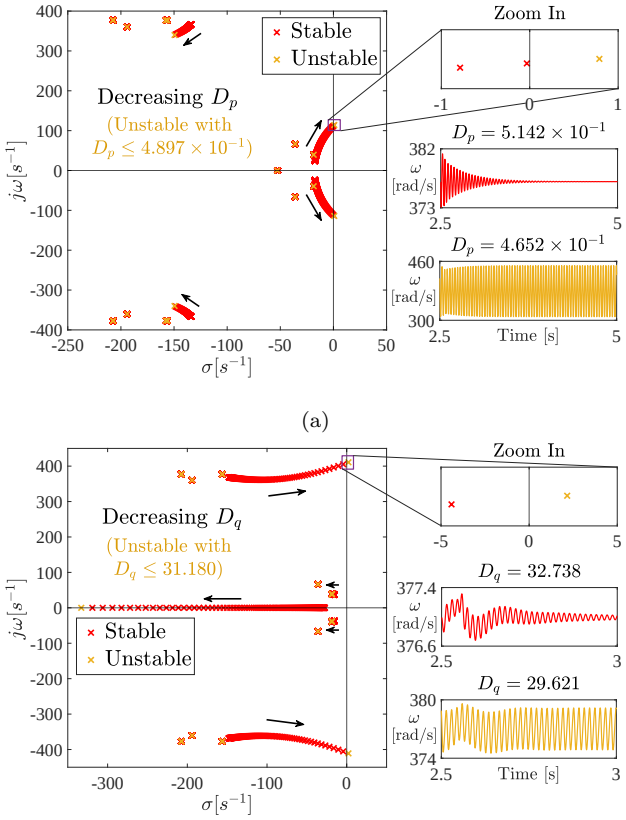

Figure 11. Small-signal model poles in the complex plane during (a) D_p gain variation and (b) D_q gain variation, and dynamic model frequency in converter 2 (synchronverter) with 10% variation around the (a) D_p limit for instability and (b) D_q limit for instability.

As can be seen in Figures 10a, 10b, 11a and 11b, the frequency behavior, obtained in the dynamic model for each selected gain, is considerably close to the results presented for the position of the poles in the complex plane, where the 10% variation around the obtained limits, made the dynamic model go from stable to the stability threshold, for the four gains analyzed. These results point to an interesting feature of the small-signal model: it represents the dynamic model conservatively, that is, the small-signal model points to microgrid instability before this actually happens in the dynamic model. Among the possibilities of representing the small-signal model, this is the best scenario, with a margin in the variation of the parameters of the dynamic model before the instability.

6. CONCLUSION

This paper proposes a modular small-signal model for different microgrid configurations. The main contributions were: the generalization of the model developed by Ferreira et al. (2019), expanding its use to a more diversified microgrid structure, enabling different configurations, and the application of this model for stability analysis of a microgrid that explores these configurations possibilities, with two converters being controlled by two different techniques (droop and synchronverter), in a microgrid operating in connected mode and with local loads.

The results obtained showed that the proposed small-signal model is applicable, properly representing the simulated dynamic model, and with a conservative representation, from the point of view of stability analysis. This evidences the possibility of application in more complex microgrids, with more elements present, in addition to being able to operate in both connected and isolated modes.

The realization of this work allowed to highlight some approaches not explored in it, which may represent relevant future contributions. Among them, it is possible to mention: the verification of the validity region of the proposed small-signal model, quantifying the deterioration away from the operating points; the use of more stability analysis tools and the possibility of doing this analysis for other microgrid parameters, such as a load change, which, in the current proposed model, requires the modification of all parameters due to the change in the operating points.

ACKNOWLEDGEMENTS

The authors would like to thank the Instituto Federal de Minas Gerais for financial support of this work.

REFERENCES

Borazjani, P., Wahab, N.I.A., Hizam, H.B., and Soh, A.B.C. (2014). A review on microgrid control techniques. In *2014 IEEE Innovative Smart Grid Technologies-Asia (ISGT ASIA)*, 749–753. IEEE.

Cao, W., Su, H., Cao, J., Sun, J., and Yang, D. (2014). Improved droop control method in microgrid and its small signal stability analysis. In *2014 International Conference on Renewable Energy Research and Application (ICRERA)*, 197–202. IEEE.

Coelho, E.A.A. (2000). *Técnicas de controle aplicadas ao paralelismo de inversores. 2000. f. 42-99.* Ph.D. thesis, Universidade Federal de Minas Gerais, UFMG, Belo Horizonte, 2000.

Coelho, E.A.A., Cortizo, P.C., and Garcia, P.F.D. (2002). Small-signal stability for parallel-connected inverters in stand-alone ac supply systems. *IEEE Transactions on Industry Applications*, 38(2), 533–542.

Ferreira, R.V., Silva, S.M., Antunes, H., and Venkataramanan, G. (2019). Dynamic analysis of grid-connected droop-controlled converters and synchronverters. *Journal of Control, Automation and Electrical Systems*, 30(5), 741–753.

Ferreira, R.V., Silva, S.M., Brandao, D.I., and Antunes, H.M. (2016). Single-phase synchronverter for residential pv power systems. In *2016 17th international conference on harmonics and quality of power (ICHQP)*, 861–866. IEEE.

Ferreira, R.V. (2019). *Comparative analysis of techniques to emulate synchronous machines in grid-connected converters.* Ph.D. thesis, Universidade Federal de Minas Gerais, UFMG, Belo Horizonte, 2019.

Konstantopoulos, G.C., Zhong, Q.C., Ren, B., and Krstic, M. (2014). Bounded droop controller for accurate load sharing among paralleled inverters. In *2014 American Control Conference*, 934–939. IEEE.

Liu, F., Liu, S., Wang, M., Zhang, Z., and Wang, H. (2020). Small-signal modeling and comparative analysis of self synchronous droop controlled inverters in microgrid system. In *2020 15th IEEE Conference on Industrial Electronics and Applications (ICIEA)*, 861–866. IEEE.

Liu, J., Miura, Y., and Ise, T. (2015). Comparison of dynamic characteristics between virtual synchronous generator and droop control in inverter-based distributed generators. *IEEE Transactions on Power Electronics*, 31(5), 3600–3611.

Rodríguez-Cabero, A., Roldan-Perez, J., and Prodanovic, M. (2017). Synchronverter small-signal modelling and eigenvalue analysis for battery systems integration. In *2017 IEEE 6th International Conference on Renewable Energy Research and Applications (ICRERA)*, 780–784. IEEE.

Saeed, M.H., Fangzong, W., Kalwar, B.A., and Iqbal, S. (2021). A review on microgrids' challenges & perspectives. *IEEE Access*, 9, 166502–166517. doi:10.1109/ACCESS.2021.3135083.

Vechiu, I., Llaria, A., Curea, O., and Camblong, H. (2011). Control of power converters for microgrids. *Compel-the International Journal for Computation and Mathematics in Electrical and Electronic Engineering - COMPEL-INT J COMPUT MATH ELEC*, 30. doi:10.1108/03321641111091575.

Vetoshkin, L. and Müller, Z. (2020). A comparative study of synchronverter stability. In *2020 21st International Scientific Conference on Electric Power Engineering (EPE)*, 1–6. IEEE.

Wandhare, R.G., Thale, S., and Agarwal, V. (2014). Design of a photovoltaic power conditioning system for hierarchical control of a microgrid. In *2014 IEEE 40th Photovoltaic Specialist Conference (PVSC)*, 3144–3149. IEEE.

Wang, S., Liu, Z., Liu, J., Boroyevich, D., and Burgos, R. (2020). Small-signal modeling and stability prediction of parallel droop-controlled inverters based on terminal characteristics of individual inverters. *IEEE Transactions on Power Electronics*, 35(1), 1045–1063. doi:10.1109/TPEL.2019.2914176.

Wei, Z., Jie, C., and Chunying, G. (2015). Small signal modeling and analysis of synchronverters. In *2015 IEEE 2nd international future energy electronics conference (IFEEC)*, 1–5. IEEE.

Yu, K., Ai, Q., Wang, S., Ni, J., and Lv, T. (2015). Analysis and optimization of droop controller for microgrid system based on small-signal dynamic model. *IEEE Transactions on Smart Grid*, 7(2), 695–705.

Zhong, Q.C., Nguyen, P.L., Ma, Z., and Sheng, W. (2014). Self-synchronized synchronverters: Inverters without a dedicated synchronization unit. *IEEE Transactions on Power Electronics*, 29(2), 617–630. doi:10.1109/TPEL.2013.2258684.

Zhong, Q.C. and Weiss, G. (2011). Synchronverters: Inverters that mimic synchronous generators. *IEEE Transactions on Industrial Electronics*, 58(4), 1259–1267. doi:10.1109/TIE.2010.2048839.

Zhou, Q., Shahidehpour, M., Paaso, A., Bahramirad, S., Alabdulwahab, A., and Abusorrah, A. (2020). Distributed control and communication strategies in networked microgrids. *IEEE Communications Surveys Tutorials*, 22(4), 2586–2633. doi:10.1109/COMST.2020.3023963.